Physica Scripta

PAPER

RECEIVED
7 September 2022

REVISED
24 December 2022

ACCEPTED FOR PUBLICATION
12 January 2023

PUBLISHED
24 January 2023

Effect of trapping in coupled kinetic Alfven-acoustic waves in a partially degenerate plasma with quantizing magnetic field

M T Asam[1], S A Bukhari[1], H A Shah[1,*], Zeeshan Iqbal[2], W Masood[3] and L Z Kahlon[1]

[1] Department of Physics, Forman Christian College, Ferozepur Road, Lahore 54600, Pakistan
[2] Department of Physics, Government College University, Katchery Road, Lahore 54000, Pakistan
[3] Department of Physics, COMSATS University, Islamabad 45550, Pakistan
[*] Author to whom any correspondence should be addressed.

E-mail: hassanshah@fccollege.edu.pk and hashah.gcl@gmail.com

Keywords: degenerate plasmas, nonlinear, solitary structures, landau quantization

Abstract

Inclusion of a quantizing magnetic field in a partially degenerate plasma has interesting effects on the propagation of solitary and nonlinear periodic structures in coupled kinetic Alfven acoustic waves. In this paper, we use two-potential theory to investigate the nonlinear structures using Sagdeev potential approach and further analyze it using nonlinear dynamical methods. It is shown that the existence of solitary structure is sensitive to small temperature effects and quantizing magnetic field in a dense plasma with adiabatically trapped electrons. The work presented here is useful in understanding the low frequency wave propagation in a dense astrophysical environment like white dwarf stars and in low beta laboratory plasmas e.g. intense laser-plasma interactions.

1. Introduction

Quantum plasmas have received much attention in the recent decades due to its presence and applications in various interesting physical domains, including but not limited to quantum dots, carbon nanotubes and micro-electronics [1–4]. Degenerate plasmas are also observed naturally in astrophysical environment such as neutron stars, white dwarfs, active galactic nuclei [5, 6] etc Linear electron oscillations in a quantum plasma have been studied in the past decade or so [7–9]. Following up on this work, Tsintsadze developed a set of fluid equations for degenerate Fermi plasmas and discussed the dispersion relations of electrostatic waves propagating in that medium [10]. Later on, nonlinear behavior of electrostatic waves in a degenerate plasma gained substantial attention, including the effect of adiabatic trapping in the propagation of solitary waves in quantum plasmas [11–14].

Trapping as a microscopic phenomenon began with the seminal paper by Gurevich [15, 16] who proposed that, in a slowly applied field, particles can get adiabatically trapped in a potential. This has a drastic effect on the number density of the trapped particles, creating a peculiar 3/2 power non-linearity rather than the usual quadratic one. Extension of the concept of trapping to quantum plasmas changes the nature of non-linearity (from $\varphi^{\frac{3}{2}}$ to $(1 + \varphi)^{\frac{3}{2}}$). Some authors have expanded $(1 + \varphi)^{\frac{3}{2}}$ expression to get an exact solution for the system, losing the fractional non-linearity in the process, to a trapping co-efficient (as in $\frac{3}{2}\varphi$) [17]. In certain cases [11–14, 18], $(1 + \varphi)^{\frac{3}{2}}$ type of non-linearity is taken as it is, and the system is investigated without expanding that expression so that the 3/2 power nonlinearity be maintained. Effect of trapping has been extensively studied in the past decade for quantum plasmas, starting with the work of Shah *et al* [11] for ion acoustic waves in a dense plasma. This work was later extended to a relativistic degenerate plasma [12] in the presence of a quantizing magnetic field [13]. Effect of trapping is also investigated for self-gravitating dusty plasma [14], and for kinetic Alfven waves (KAWs) in the classical case [19] and later for a fully degenerate plasma [18]. Recently, adiabatic trapping was investigated in a dissipative medium for ion acoustic waves in a magnetized plasma, where Burgers equation was derived, and nonlinear shock wave formation of different kinds was observed [20]. 3D propagation of such waves was also studied recently in a homogeneous multi-ion magnetized quantum plasma [21].

Most of the work for the effect of trapping in quantum plasmas for low frequency regimes is done for electrostatic waves, even in the presence of the quantizing and super-strong magnetic fields [11–14, 17, 18, 22]. Since most dense astrophysical environments have a strong ambient magnetic field, investigating the effect of trapping in coupled kinetic Alfven-acoustic waves (CKAAWs) may yield more practical results. In this paper, two-potential theory [23] is used to investigate nonlinear CKAAWs in degenerate plasmas. This theory is valid for a low frequency ($\omega^2 \ll \omega_{ci}^2$) and low beta plasma. Previously, finite amplitude solitary structures in CKAAWs were studied using the two-potential theory with Maxwellian distribution [24, 25] and later with adiabatic trapping in a classical plasma [19]. Lately, much promising work is still ongoing for the propagation of KAWs in non-Maxwellian kappa distributed electrons in space and upper atmospheric plasma [26, 27], but not much is done for the aforementioned waves in quantum plasmas or dense astrophysical plasmas. This concept was extended by Sabeen *et al* [18] to quantum plasmas, where solitary structures were investigated for CKAAWs in a fully degenerate plasma.

The presence of a sufficiently strong magnetic field leads to Landau quantization [16], whereby the magnetic field of electrons are quantized and the magnetic field affects the electron dynamics, even if only parallel propagating waves are considered.

In this paper, we will discuss the effect of trapping in nonlinear CKAAWs for a partially degenerate plasma in the presence of quantizing magnetic field [13, 22]. In section II, the basic set of equations is discussed, and the linear dispersion relation is derived. In section III, non-linear properties of the system are observed using the Sagdeev potential approach. In section IV, both solitary and non-linear periodic structures are investigated using dynamical system analysis. Using fixed points-analysis, we determine the nature of waves that may propagate in such a system [28, 29]. Section V contains results and discussions.

2. Mathematical preliminaries and linear analysis

In the present section, we begin by briefly introducing the two-potential theory [23] This approach is valid for low β plasmas only ($1 > \beta > m_e/m_i$). In the case of quantum plasmas the plasma β is defined as $\beta_f = \frac{2c_{sf}{}^2}{v_A{}^2}$, where $c_{sf} = \sqrt{\frac{\varepsilon_f}{m_i}}$ is the ion acoustic velocity for a quantum plasma, m_i is the ion mass, $v_A = \frac{B_0}{\sqrt{\mu_0 m_i n_0}}$ is the Alfven velocity and μ_0 is the magnetic permeability constant . We consider motion in the x–z direction, taking B_0 in the z direction and further by using the two -potential theory, the electric field $\boldsymbol{E}$ is represented in terms of two potentials φ and Φ in the following manner [23],

$$E_x = -\frac{\partial \Phi}{\partial x}, \quad E_z = -\frac{\partial \varphi}{\partial z}, \quad E_y = 0\,, \quad B_z = B_0$$

Using the effect of adiabatic trapping in a dense plasma and keeping the effects of temperature and quantizing magnetic field into account, the number density of partially degenerate electrons using Fermi–Dirac statistics [13] is given as,

$$n = \frac{3}{2}\eta(1+\Psi)^{\frac{1}{2}} + (1+\Psi-\eta)^{\frac{3}{2}} - \eta\frac{T^2}{2}(1+\Psi)^{-\frac{3}{2}} + T^2(1+\Psi-\eta)^{-\frac{1}{2}} \tag{1}$$

Where the potential Ψ is normalized as, $\Psi = \frac{e\varphi}{\varepsilon_f}$ and the temperature is normalized as, $T = \frac{\pi T_0}{2\sqrt{2}\varepsilon_f}$, where T_0 is the ambient temperature in energy units. Fermi energy is given by $\varepsilon_f = \frac{\hbar^2(3\pi^2 n_0)^{\frac{2}{3}}}{2m_e}$, the effect of quantizing magnetic field is given through the parameter $\eta = \frac{\hbar\omega_{ce}}{\varepsilon_f}$, $\omega_{ce} = \frac{eB_0}{m_e}$ is the electron cyclotron frequency, B_0 represents the ambient magnetic field, which is a constant and the number density is normalized as $n = \frac{n_e}{n_{e0}}$, where n_{e0} is the background number density.

Ions are treated classically due to their heavy mass ($m_i \gg m_e$) and, therefore, the equation of motion of ions is taken to be classical in nature. Thus, the ion equation of motion for the case of low beta plasma is given by,

$$m_i\left(\frac{\partial \boldsymbol{v_i}}{\partial t} + (\boldsymbol{v_i}.\nabla)\boldsymbol{v_i}\right) = e(\boldsymbol{E} + \boldsymbol{v_i} \times \boldsymbol{B}_0) \tag{2}$$

The Ampere's law, modified with the two-potential theory, gives us [19],

$$\frac{\partial^4}{\partial z^2 \partial x^2}(\Phi - \varphi) = \mu_0 \frac{\partial^2}{\partial t \partial z} j_z \tag{3}$$

Here j_z is the current density.

The ion continuity equation, in the given geometry reads as,

$$\frac{\partial n}{\partial t} + \frac{\partial}{\partial x}(nv_x) + \frac{\partial}{\partial z}(nv_z) = 0 \quad (4)$$

From the electron continuity equation, we obtain the expression for the current density in z direction, which can be expressed as,

$$\frac{\partial j_z}{\partial z} = e\frac{\partial n}{\partial t} + e\frac{\partial}{\partial z}(nv_z) \quad (5)$$

Linearizing the above set of equations and solving them simultaneously by using a plane wave solution gives us the following linear dispersion relation for CKAAWs,

$$\left(1 - \frac{v_A{}^2 k_z{}^2}{\omega^2}\right)\left((1 + T^2)\frac{3}{4}\eta + \frac{3}{2}(1-\eta)^{\frac{1}{2}} - \frac{T^2}{2}(1-\eta)^{-\frac{3}{2}} - \frac{c_{sf}{}^2 k_z{}^2}{\omega^2}\right) = \frac{\lambda_{sf} v_A{}^2 k_z{}^2}{\omega^2} \quad (6)$$

Where λ_{sf} is the coupling parameter and is defined as $\lambda_{sf} = \frac{c_{sf}{}^2 k_x{}^2}{\Omega_i{}^2}$, where $\Omega_i = \frac{eB_0}{m_i}$ is the ion cyclotron frequency. Here

$$k_x = k \sin\theta, \quad k_x = k\cos\theta$$

Where θ is the angle between ambient magnetic field and propagation vector.

It is clear from the linear dispersion relation of CKAAWs for partially degenerate and magnetically quantized plasma that, for very high values of plasma beta $\left(\beta_f = \frac{2c_{sf}{}^2}{v_A{}^2}\right)$, v_A becomes insignificant in equation (6) and we are left with ion acoustic mode only.

We note that here $\eta < 1$ is taken for strong magnetic fields and $\eta > 1$ is taken for super-strong magnetic fields, which is not considered here and is beyond the scope of the present work.

If we put the normalized temperature and quantizing magnetic field to be equal to zero, we retrieve the linear dispersion for a fully degenerate plasma, in accordance with Sabeen *et al* [18]. Unlike the classical cases, the effect of trapping remains visible as a $3/2$ coefficient in the linear dispersion relation as well. The coupling term appears on the right-hand side of equation (6). In the limiting case of $k_x = 0$, equation (6) decouples and gives us the linear dispersion relations for the ion acoustic waves and Alfven waves. In the next section, we shall investigate the nonlinear behavior of CKAAWs.

3. Non-linear behavior and Sagdeev potential

Due to the nature of nonlinearity in the system of equations, it is not possible to find the exact solution. One may expand the non-linear terms into leading orders, in terms of the potential Ψ, but because of such an approximation, the fractional nature of nonlinearity is lost. Retaining the fractional non-linearity makes it impossible to find the exact solution of the system, therefore, we use the Sagdeev potential method to investigate the allowed regions of solitary wave propagation and nonlinear periodic waves. We shift to the co-moving frame of reference, which is defined as,

$$\alpha = K_x x + K_z z - Mt$$

Here K_x and K_z are the directional cosines, The condition for directional cosines is $K_x{}^2 + K_z{}^2 = 1$; where $K_x = \sin\theta$ and $K_z = \cos\theta$. We have used the following normalized parameters, $M = \frac{u}{c_{sf}}$, $n = \frac{n}{n_o}$, $t = \Omega_i t$ and $v = \frac{v}{c_{sf}}$. Thenceforth, the dimensionless form of the system of equations is as follows,

$$-M\frac{\partial v_z}{\partial \alpha} + K_x v_x \frac{\partial v_z}{\partial \alpha} + K_z v_z \frac{\partial v_z}{\partial \alpha} = -K_z \frac{\partial \Psi}{\partial \alpha} \quad (7)$$

$$v_x = MK_x \frac{\partial^2 \Phi}{\partial \alpha^2} \quad (8)$$

$$2K_x{}^2 K_z{}^2 \frac{\partial^4}{\partial \alpha^4}(\Phi - \Psi) = \beta_f\left(M^2 \frac{\partial^2 n}{\partial \alpha^2} - MK_z \frac{\partial^2}{\partial \alpha^2} n v_z\right) \quad (9)$$

$$-M\frac{\partial n}{\partial \alpha} + K_x \frac{\partial (nv_x)}{\partial \alpha} + K_z \frac{\partial (nv_z)}{\partial \alpha} = 0 \quad (10)$$

Integrating equation (7) using the boundary conditions that as $\alpha \to \infty$, the perturbed quantities v, Φ, $\Psi \to 0$ and the number density $n \to A$, yields

$$MA\frac{\partial v_z}{\partial \alpha} = K_z n\frac{\partial \Psi}{\partial \alpha} \tag{11}$$

Where A is the integration constant given by

$$A = \frac{3}{2}\eta + (1-\eta)^{\frac{3}{2}} + T^2(1-\eta)^{-\frac{1}{2}}$$

Here it is worth noting that, all the terms with η^2T^2, ηT^2, η^2T^4, T^4 and η^2 are ignored since for a quantum plasma η, $T < 1$ and such terms will have little to no contribution to the results. Plugging the value of equation (1) in equation (11) and integrating once gives,

$$MAv_z = K_z\left(\eta(1+\Psi)^{\frac{3}{2}} + \frac{2}{5}(1+\Psi-\eta)^{\frac{5}{2}} + 2T^2(1+\Psi-\eta)^{\frac{1}{2}} - B\right) \tag{12}$$

Where the integration constant B is given by

$$B = \eta + \frac{2}{5}(1-\eta)^{\frac{5}{2}} + 2T^2(1-\eta)^{\frac{1}{2}}$$

Using equation (10), and integrating once and using the boundary conditions given above, we obtain

$$v_x = \frac{M}{K_x}\left(1 - \frac{A}{n}\right) - \frac{K_z v_z}{K_x} \tag{13}$$

Integrating equation (9) twice and then using equation (12) gives

$$\frac{\partial^2\Psi}{\partial\alpha^2} = \frac{v_x}{K_X M} - \frac{\beta_f}{2{K_x}^2{K_z}^2}[M^2(n-A) - MK_z n v_z] \tag{14}$$

Substituting the values of equations (2), (12) and (13) in equation (14) gives us,

$$\begin{aligned}{K_X}^2\frac{\partial^2\Psi}{\partial\alpha^2} = {} & 1 - A\left((1+\Psi-\eta)^{-\frac{3}{2}} - \frac{3}{2}\eta(1+\Psi)^{-\frac{5}{2}} - T^2(1+\Psi-\eta)^{-\frac{7}{2}}\right)\\ & -\frac{{K_z}^2\beta_f}{2M_A^2A}\left(\eta(1+\Psi)^{\frac{3}{2}} + \frac{2}{5}(1+\Psi-\eta)^{\frac{5}{2}} + 2T^2(1+\Psi-\eta)^{\frac{1}{2}} - B\right)\\ & -\frac{M_A^2}{{K_z}^2}\left(\frac{3}{2}\eta(1+\Psi)^{\frac{1}{2}} + (1+\Psi-\eta)^{\frac{3}{2}} + T^2(1+\Psi-\eta)^{-\frac{1}{2}} - A\right)\\ & -\frac{\beta_f}{2A}\left(\frac{8}{5}\eta(1+\Psi)^3 + \frac{2}{5}(1+\Psi-\eta)^4 + \frac{12}{5}T^2(1+\Psi-\eta)^2\right.\\ & \left. -B\left((1+\Psi-\eta)^{\frac{3}{2}} + \frac{3}{2}\eta(1+\Psi)^{\frac{1}{2}} + T^2(1+\Psi-\eta)^{-\frac{1}{2}}\right)\right)\end{aligned} \tag{15}$$

In the above expression, we have Taylor expanded the $1/n$ term with respect to temperature and ignored the higher order terms. Moreover, we have used the Alfvenic Mach number which is defined as ${M_A}^2 = \frac{1}{2}\beta_f M^2$ and is the ratio of the speed of wave to the Alfven velocity. We express equation (15) through the Sagdeev potential $V(\Psi)$ in the usual manner [11],

$$\frac{\partial^2\Psi}{\partial\alpha^2} = -\frac{\partial V}{\partial\Psi} \tag{16}$$

Integrating equation (16) gives,

$$\begin{aligned}V(\Psi) = {} & -\frac{1}{{K_X}^2}\left[\Psi + A\left(2(1+\Psi-\eta)^{-\frac{1}{2}} - \eta(1+\Psi)^{-\frac{3}{2}} - \frac{2}{5}T^2(1+\Psi-\eta)^{-\frac{5}{2}}\right)\right.\\ & -\frac{{K_z}^2\,\beta_f}{2\,M_A^2A}\left(\frac{2}{5}\eta(1+\Psi)^{\frac{5}{2}} + \frac{4}{35}(1+\Psi-\eta)^{\frac{7}{2}} + \frac{4}{3}T^2(1+\Psi-\eta)^{\frac{3}{2}} - \Psi B\right)\\ & -\frac{M_A^2}{{K_z}^2}\left(\eta(1+\Psi)^{\frac{3}{2}} + \frac{2}{5}(1+\Psi-\eta)^{\frac{5}{2}} + 2T^2(1+\Psi-\eta)^{\frac{1}{2}} - \Psi A\right)\\ & +\frac{\beta_f}{2\,A}\left(\frac{2}{5}\eta(1+\Psi)^4 + \frac{2}{25}(1+\Psi-\eta)^5 + \frac{4}{5}T^2(1+\Psi-\eta)^3\right.\\ & \left.\left. -B\left(\eta(1+\Psi)^{\frac{3}{2}} + \frac{2}{5}(1+\Psi-\eta)^{\frac{5}{2}} + 2T^2(1+\Psi-\eta)^{\frac{1}{2}}\right)\right) + C\right]\end{aligned} \tag{17}$$

Where, C is the constant of integration, which is found by using the standard boundary condition [11], $V(\Psi) \to 0$, when $\Psi \to 0$ and is given by,

$$C = \frac{1}{{K_X}^2}\left[A\left(2(1-\eta)^{-\frac{1}{2}} - \eta - \frac{2}{5}T^2(1-\eta)^{-\frac{5}{2}}\right)\right.$$
$$-\frac{{K_z}^2\beta_f}{2\,M_A^2 A}\left(\frac{2}{5}\eta + \frac{4}{35}(1-\eta)^{\frac{7}{2}} + \frac{4}{3}T^2(1-\eta)^{\frac{3}{2}}\right)$$
$$-\frac{M_A^2}{{K_z}^2}\left(\eta + \frac{2}{5}(1-\eta)^{\frac{5}{2}} + 2T^2(1-\eta)^{\frac{1}{2}}\right)$$
$$+\frac{\beta_f}{2A}\left(\frac{2}{5}\eta + \frac{2}{25}(1-\eta)^5 + \frac{4}{5}T^2(1-\eta)^3\right.$$
$$\left.\left.-B\left(\eta + \frac{2}{5}(1-\eta)^{\frac{5}{2}} + 2T^2(1-\eta)^{\frac{1}{2}}\right)\right)\right] \quad (18)$$

In order to carry out numerical and graphical analysis of our results of the section above, we use the data from the precincts of white dwarf stars [30]. It is believed that in the outer shells of supernovae, electrostatic structures may exist [31]. Studying electromagnetic waves in such dense plasmas may have more interesting outcomes in the future. We now examine nonlinear CKAAWs with adiabatically trapped electrons in the presence of quantizing magnetic field, numerically. For the above-mentioned model, we have plotted the effective Sagdeev potential, phase portraits and corresponding structures.

We find the range of mach number for which solitary waves exist. This is determined numerically for $n_0 = 1.8 \times 10^{32}\ \mathrm{m}^{-3}$, $B_0 = 1 \times 10^6\mathrm{T}$, $\theta = 75^\circ$. It is found that both compressive and rarefactive solitary waves are obtained for $0.05 \leqslant M_A \leqslant 0.07$ and $0.18 \leqslant M_A \leqslant 0.24$, and only rarefactive solitary structures are obtained for $0.08 \leqslant M_A \leqslant 0.17$ as shown in figure 1(a). This shows that CKAAWs under the given conditions is a sub-Alfvenic wave. The variation of Sagdeev potential over the complete range of Alfvenic Mach number is clear in 3-dimensional plot as seen in figure 1(b).

It is observed that for the existence of solitary structure the range of Alfvenic Mach number strongly depends on the angle of propagation. As we increase the angle of propagation, the range of Alfvenic Mach number narrows down. For $\theta = 85^\circ$, the range of Mach number is from $M_A = 0.015$ to $M_A = 0.085$ and for $\theta = 86^\circ$, the range of Alfvenic Mach number decreases and is from $M_A = 0.012$ to $M_A = 0.068$. Figure 2 shows that at $M_A = 0.07$ the depth of Sagdeev potential decreases at 85° and $\theta = 86^\circ$ in comparison to 75°.

It is noted that the solitary structures are only found for a specific value of parameters and for the other values, we have observed the existence of nonlinear periodic waves. This behavior was also investigated by Yu *et al* where solitary KAWs were studied in a classical plasma [25].

4. Dynamical analysis

In this section, we investigate the non-linear wave propagation using dynamical system analysis. The significance of using this method is that it helps in understanding the wave trajectory in phase space and such trajectories provide information about the solution. Dynamical equations corresponding to ordinary differential equation (15) are as follows

$$\left[\begin{array}{l}\dot{\Psi} = \dfrac{\partial\Psi}{\partial\alpha} = z \\ \dot{z} = \dfrac{\partial z}{\partial\alpha} = \dfrac{\partial^2\Psi}{\partial\alpha^2}\end{array}\right. \quad (19)$$

Where $\frac{\partial^2\Psi}{\partial\alpha^2}$ is given in equation (15). We write the Hamiltonian for this dynamical system as

$$H(z, \Psi) = \frac{z^2}{2} - \frac{1}{{K_X}^2}\left[\Psi + A\left(2(1+\Psi-\eta)^{-\frac{1}{2}} - \eta(1+\Psi)^{-\frac{3}{2}} - \frac{2}{5}T^2(1+\Psi-\eta)^{-\frac{5}{2}}\right)\right.$$
$$-\frac{{K_z}^2\beta_f}{2\,M_A^2 A}\left(\frac{2}{5}\eta(1+\Psi)^{\frac{5}{2}} + \frac{4}{35}(1+\Psi-\eta)^{\frac{7}{2}} + \frac{4}{3}T^2(1+\Psi-\eta)^{\frac{3}{2}} - B\Psi\right)$$
$$-\frac{M_A^2}{{K_z}^2}\left(\eta(1+\Psi)^{\frac{3}{2}} + \frac{2}{5}(1+\Psi-\eta)^{\frac{5}{2}} + 2T^2(1+\Psi-\eta)^{\frac{1}{2}} - A\Psi\right)$$
$$+\frac{\beta_f}{2A}\left(\frac{2}{5}\eta(1+\Psi)^4 + \frac{2}{25}(1+\Psi-\eta)^5 + \frac{4}{5}T^2(1+\Psi-\eta)^3\right.$$
$$\left.\left.-B\left(\eta(1+\Psi)^{\frac{3}{2}} + \frac{2}{5}(1+\Psi-\eta)^{\frac{5}{2}} + 2T^2(1+\Psi-\eta)^{\frac{1}{2}}\right)\right) + C\right] \quad (20)$$

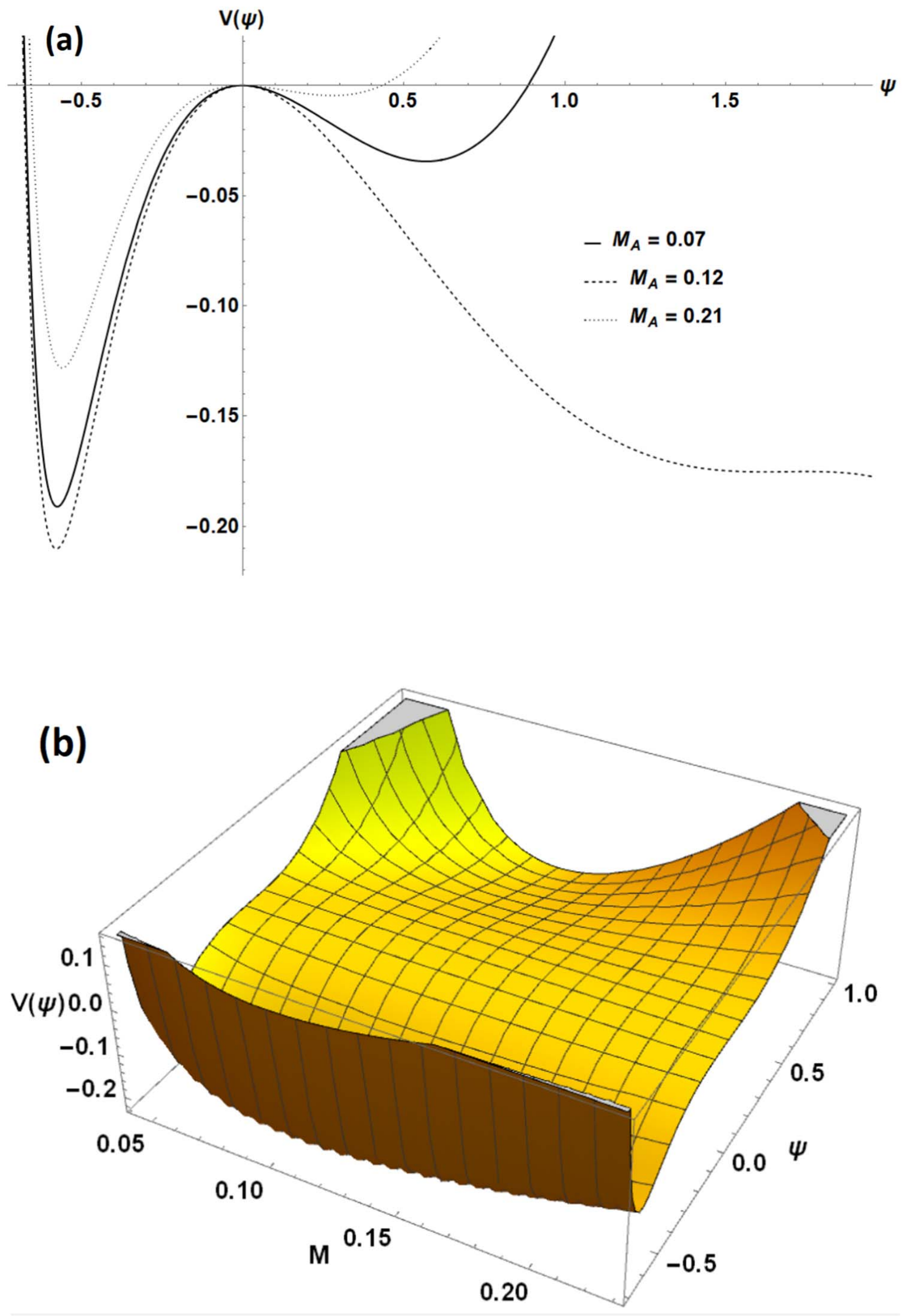

Figure 1. Solitary structure for $n_0 = 1.8 \times 10^{32}$ m^{-3}, $B_0 = 1 \times 10^6$ T, $\theta = 75°$ and $T = 0.24$. (a) Sagdeev potential different for values of Alfvenic Mach No. (b) 3-dimensional plot of Sagdeev Potential over the complete the complete range of Alfvenic Mach Number.

The value of constant C is given in equation (18). The second term in Hamiltonian shows effective potential [32] which in our case is the Sagdeev potential given in equation (17). The dynamical system in equation (19) comprises of transcendental equations. In order to solve nonlinear equations for the fixed point, we opt for the numerical approach.

The Jacobian matrix of dynamical system in equation (19) gives eigenvalues and is given by

$$J = \begin{pmatrix} 0 & 1 \\ P & 0 \end{pmatrix} \tag{21}$$

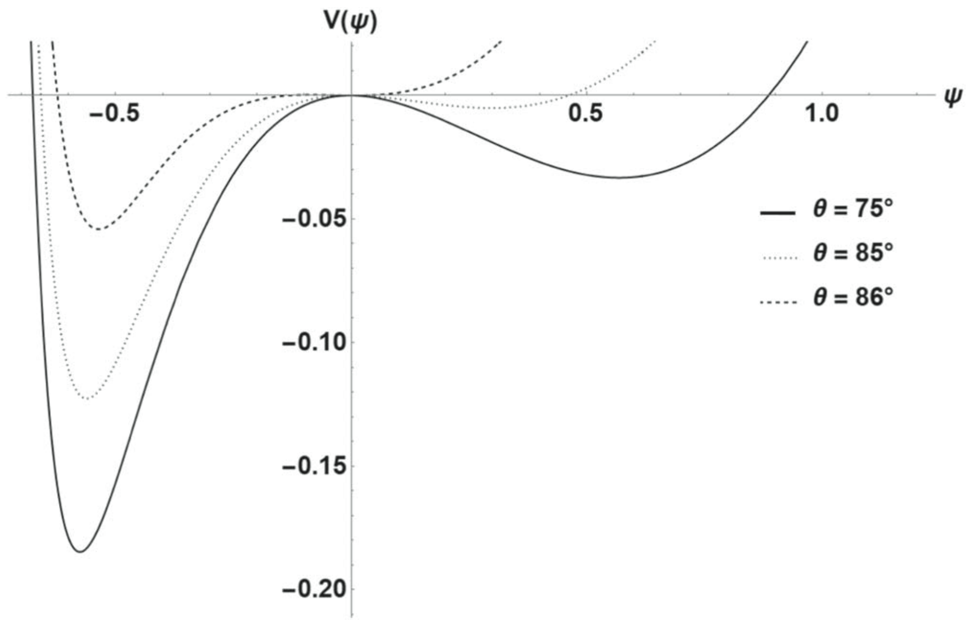

Figure 2. Sagdeev potential for different value of angles at $n_0 = 1.8 \times 10^{32}\ \mathrm{m}^{-3}$, $B_0 = 1 \times 10^6$ T, $M_A = 0.07$ and $T = 0.24$.

Where

$$P = \frac{\partial}{\partial\Psi}\left(\frac{\partial^2\Psi}{\partial\alpha^2}\right)$$

$$\begin{aligned} P = \frac{1}{K_X{}^2}\Bigg[& -A\left(-\frac{3}{2}(1+\Psi-\eta)^{-\frac{5}{2}} + \frac{15}{4}\eta(1+\Psi)^{-\frac{7}{2}} + \frac{7}{2}T^2(1+\Psi-\eta)^{-\frac{9}{2}}\right) \\ & -\frac{K_z{}^2\,\beta_f}{2\,M_A^2 A}\left(\frac{3}{2}\eta(1+\Psi)^{\frac{1}{2}} + (1+\Psi-\eta)^{\frac{3}{2}} + T^2(1+\Psi-\eta)^{-\frac{1}{2}}\right) \\ & -\frac{M_A^2}{K_z{}^2}\left(\frac{3}{4}\eta(1+\Psi)^{-\frac{1}{2}} + \frac{3}{2}(1+\Psi-\eta)^{\frac{1}{2}} - \frac{T^2}{2}(1+\Psi-\eta)^{-\frac{3}{2}}\right) \\ & -\frac{\beta_f}{2A}\Bigg(\frac{24}{5}\eta(1+\Psi)^2 + \frac{8}{5}(1+\Psi-\eta)^3 + \frac{24}{5}T^2(1+\Psi-\eta) \\ & -B\left(\frac{3}{2}(1+\Psi-\eta)^{\frac{1}{2}} + \frac{3}{4}\eta(1+\Psi)^{-\frac{1}{2}} - \frac{T^2}{2}(1+\Psi-\eta)^{-\frac{3}{2}}\right)\Bigg)\Bigg] \end{aligned} \tag{22}$$

If 'I' is the identity matrix, then the characteristics equation is given as

$$det(J - \lambda I) = 0$$

Using equation (21) in characteristic equation, we get the required eigenvalues

$$\begin{vmatrix} -\lambda & 1 \\ P & -\lambda \end{vmatrix} = 0$$

$$\Rightarrow \lambda_{a,b} = \pm\sqrt{P} \tag{23}$$

Here, the eigenvalues are again calculated numerically for different values of η, M_A, K_x, K_z and T by keeping the normalized density and background magnetic field constant. We get different eigen values for different equilibrium points. It is clear from equation (23) that if $P < 0$ for a given equilibrium point, we get centers and for $P > 0$, we obtain saddle points [33].

Using the above-mentioned dynamical system, we first plot the phase portraits (equation 19) for different values of the Mach number. We obtain homoclinic orbits (Thick black line) for $M_A = 0.1$ and $M_A = 0.2$, corresponding to solitary structure as seen in figures 3(a) and (b) respectively. The closed orbits within these homoclinic orbits show nonlinear periodic waves. For these trajectories, equilibrium or fixed points have been calculated numerically. Eigenvalues for the equilibrium or fixed points are also calculated numerically using equation (22). Figure 3(a) shows rarefactive solitary structure for $M_A = 0.1$. Eigenvalues show that fixed point (0, 0) is a saddle point and fixed point (−0.586 13, 0) is a center. Figure 3(b) shows both compressive and

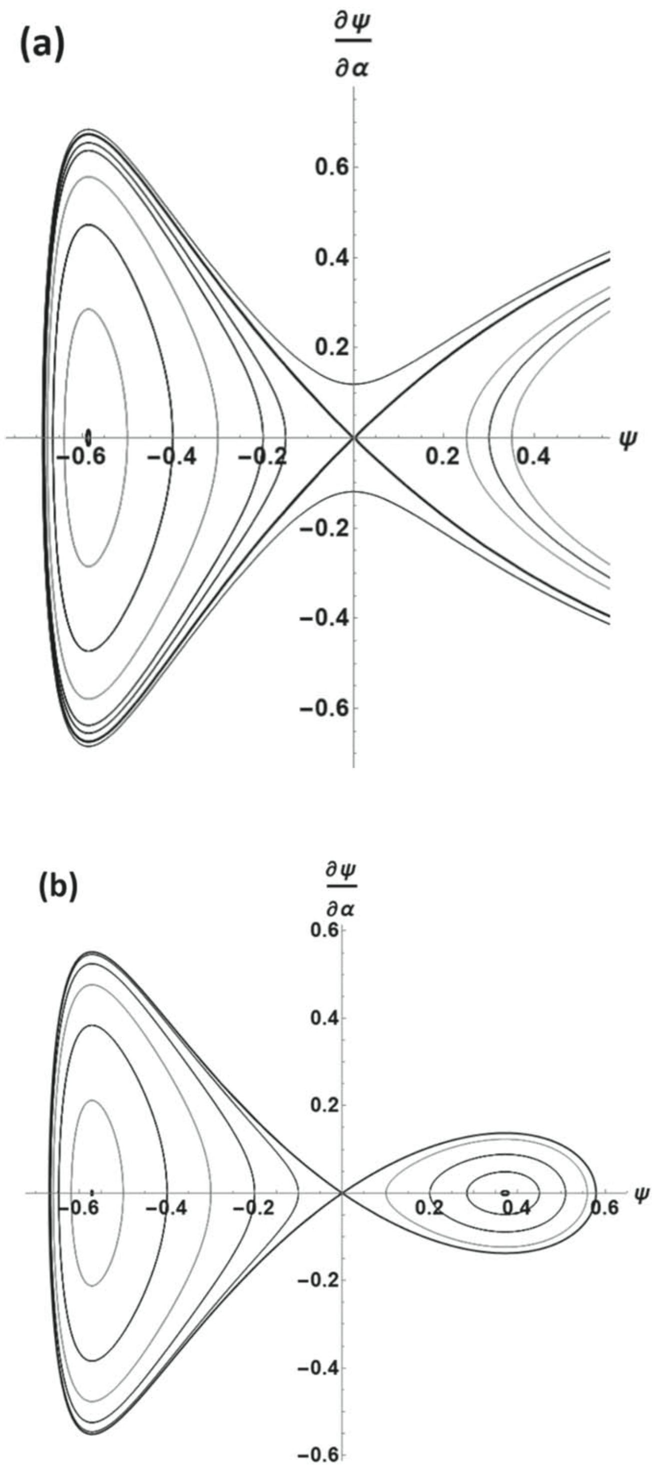

Figure 3. Phase portraits for $n_0 = 1.8 \times 10^{32}\ \mathrm{m}^{-3}$, $B_0 = 1 \times 10^6$ T, $\theta = 75°$ and $T = 0.24$. (a) For $M_A = 0.1$ (b) For $M_A = 0.2$.

rarefactive solitary structures for $M_A = 0.2$. Eigenvalues for these equilibrium points using equation (22) show that fixed point (0, 0) is a saddle point and fixed points (−0.571 38, 0) and (0.371 84, 0) are centers.

It is observed that for given values of density and magnetic field, we get a particular temperature for which solitary structure exists. Once solitary structure forms, it sustains itself only for the variation of Alfvenic Mach number M_A and not for any variation of other parameters. We note that Yu and Shukla [25] have examined the conditions for existence of solitary structures for KAWs and have shown that solitary KAWs exist only for specific values of parameters in the classical plasma as well. In case of e–p–i plasma, Kakati and Goswami [34] also investigated the existence conditions for solitary KAWs. In the present case when $n_0 = 1.8 \times 10^{32}\ \mathrm{m}^{-3}$, $B_0 = 1 \times 10^6$T, we get $T = 0.24$ for which solitary structure exists. For $0.24 < T \leqslant 0.35$ and $0 \leqslant T < 0.24$ we obtain homoclinic orbits which corresponds to non-linear pulses. For $T > 0.35$, we get periodic waves only.

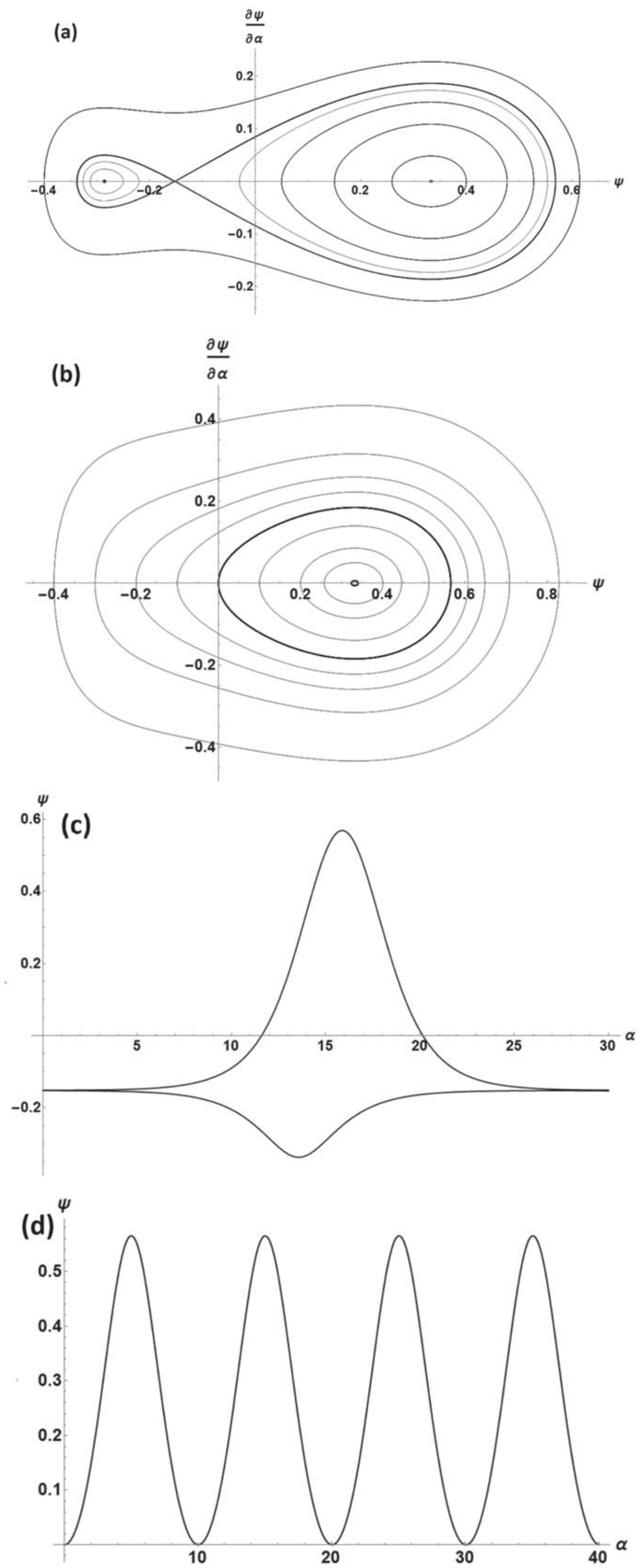

Figure 4. Dynamical plots for $n_0 = 1.8 \times 10^{32}$ m^{-3}, $B_0 = 1 \times 10^6$ T, $\theta = 75°$ and $M_A = 0.06$. (a) Homoclinic orbits at $T = 0.35$ (b) Periodic orbits at $T = 0.4$ (c) Nonlinear pulses at $T = 0.35$ corresponding to figure 1(a). (d) The corresponding periodic wave profile at $T = 0.4$.

Phase plot (from equation 19) in figure 4(a) shows a homoclinic orbit enclosing non-linear periodic orbits for $T = 0.35$. Eigenvalues for these equilibrium points using equation (22) show that fixed point $(-0.152\,52, 0)$ is a saddle point and $(-0.285\,65, 0)$ and $(0.332\,99, 0)$ are centers. Figure 4(b) shows only periodic orbits for

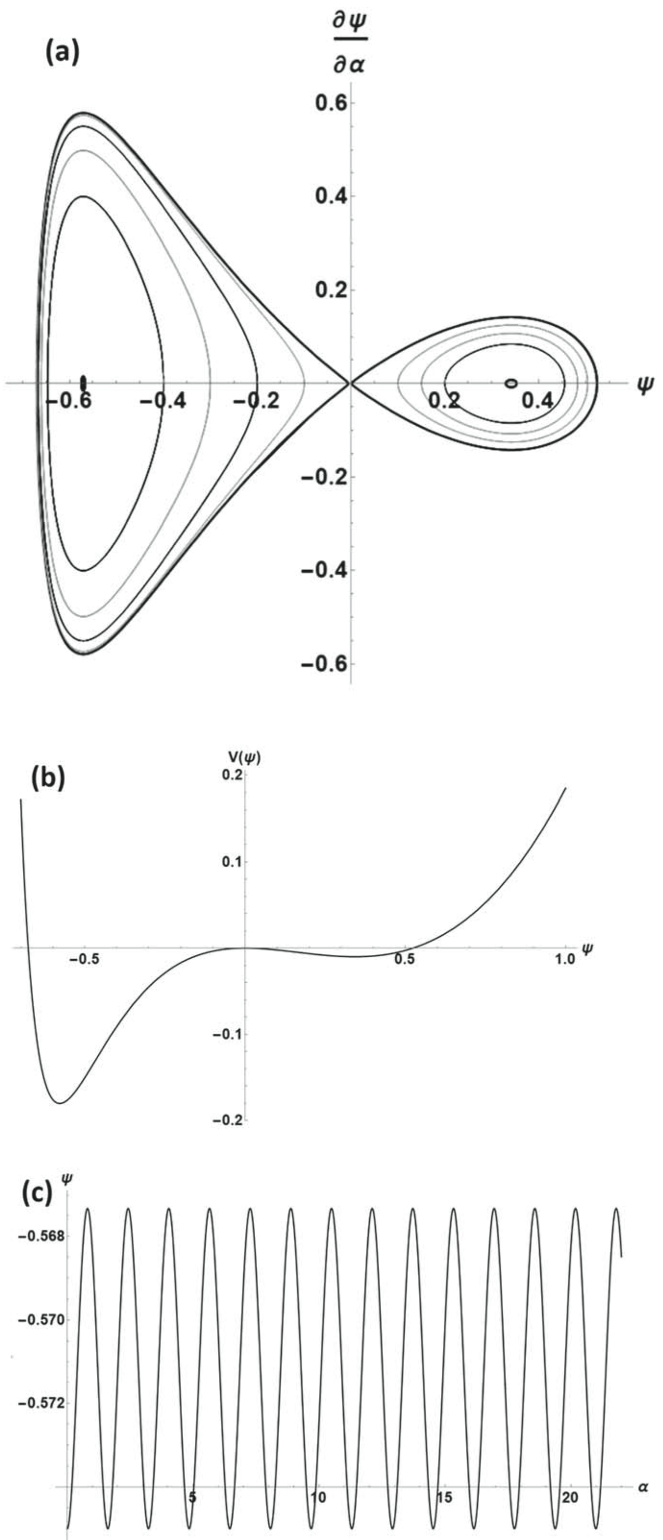

Figure 5. (a) Phase portrait at $\eta = 0.1$ for $n_0 = 1.8 \times 10^{32}$ m^{-3}, $B_0 = 1 \times 10^6$ T, $\theta = 75°$ and $M_A = 0.06$. (b) Effective potential $V(\Psi)$ versus Ψ. (c) The periodic wave profile corresponding to (a) and (b).

nonlinear periodic waves with center at (0.331 63, 0). For $T = 0.35$ and $T = 0.4$, the corresponding amplitude profiles are shown in figures 4(c) and (d), respectively.

Phase portrait of dynamical system in equation (19) for different values of quantizing magnetic fields gives homoclinic orbits, enclosing the periodic orbits. At $\eta = 0.1$, for background density $n_0 = 1.8 \times 10^{32}$ m^{-3}, magnetic field $B_0 = 1 \times 10^6$T, normalized temperature $T = 0.24$, Alfvenic mach number $M_A = 0.06$ and angle of propagation is $\theta = 75°$.we get homoclinic trajectory, which is corresponding to the solitary structure in figure 5(a). Eigenvalues using equation (23) show that fixed point (0, 0) is a saddle point and fixed points

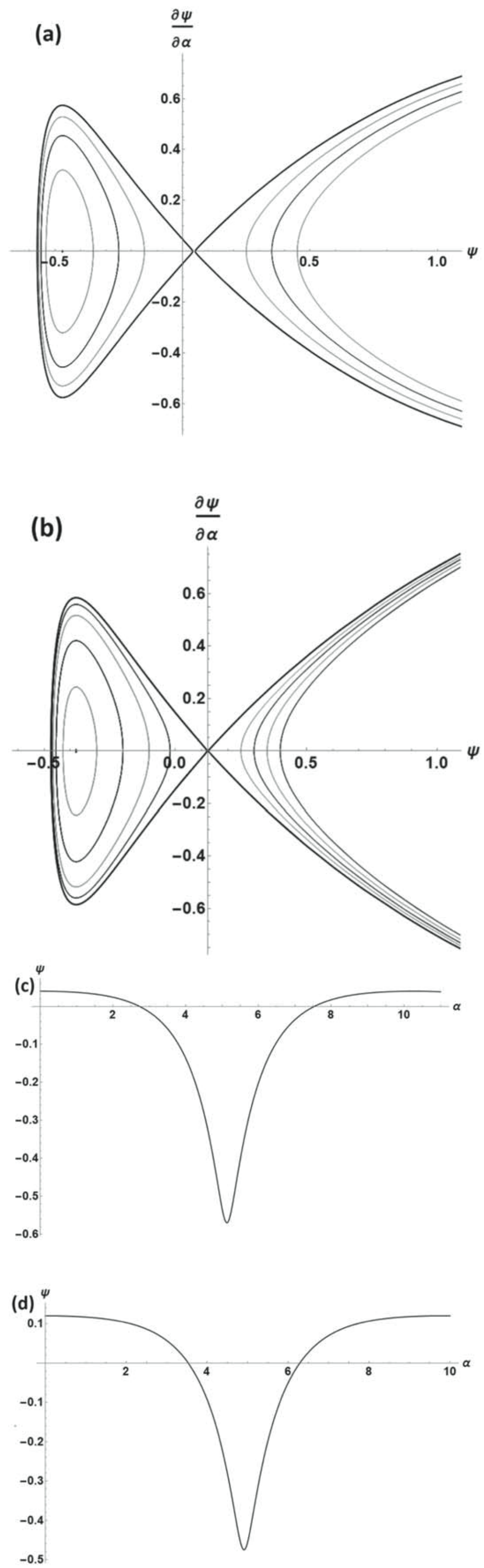

Figure 6. (a) Phase portrait at $\eta = 0.2$ (b) phase portrait at $\eta = 0.3$ (c) Nonlinear pulses at $\eta = 0.2$ corresponding to figure 6(a) (d) Nonlinear pulses at $\eta = 0.3$ corresponding to figure 6(b). For $n_0 = 1.8 \times 10^{32}$ m^{-3}, $B_0 = 1 \times 10^6$ T, $\theta = 75°$ and $M_A = 0.06$.

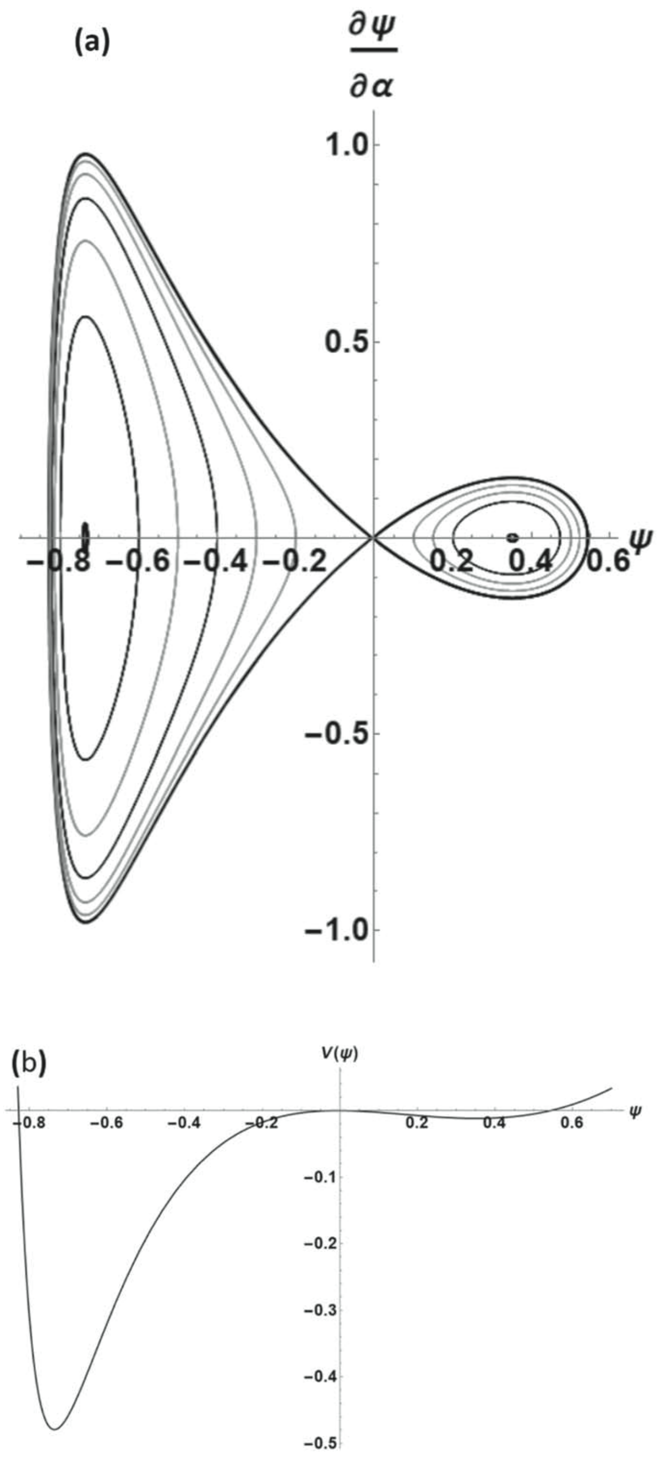

Figure 7. (a) Phase portrait at $\eta = 0$ for $n_0 = 1.8 \times 10^{32}$ m^{-3}, $B_0 = 1 \times 10^6$ T , $\theta = 75°$ and $M_A = 0.06$. (b) Effective potential $V(\Psi)$ versus Ψ.

$(-0.5537, 0)$ and $(0.3407, 0)$ are centers. We get both compressive and rarefactive solitary structures that can clearly be shown in the phase portraits and Sagdeev potential $V(\Psi)$ profiles in figures 5(a) and (b), respectively. Figure 5(c) shows one of the corresponding time series of the plots of figure 5(a).

In figures 6(a), (b), we see the variation in phase portrait and corresponding structures for quantizing magnetic field when and $\eta = 0.3$. For a fixed value of n_0, M_A, T and θ we note that the increase in η is a result of the increasing ambient magnetic field B_0. ,we get a homoclinic trajectory in phase portrait of dynamical system. When $\eta = 0.2$, fixed point $(0.0456, 0)$ is a saddle point and fixed point $(-0.4785, 0)$ is a center in figure 6(a). Figure 6(b) shows When $\eta = 0.3$, fixed point $(0.1247, 0)$ is a saddle point and fixed point $(-0.3786, 0)$ is a center. Amplitude profiles for $\eta = 0.2$ and $\eta = 0.3$ show nonlinear pulses in figures 6(c), (d).

In the absence of quantizing magnetic field, we again get homoclinic trajectory corresponding to solitary structure as shown in figure 7(a). In that case, the fixed point (0, 0) is a saddle point and fixed points (−0.735 66,0) and (0.351 76, 0) are centers. Both compressive and rarefactive solitary structures are obtained that can clearly be shown in phase portrait and Sagdeev potential $V(\Psi)$ profiles in figures 7(a) and (b), respectively.

It is also examined that for fully degenerate plasma ($T = 0$) and in the absence of quantizing magnetic field ($\eta = 0$), we retrieve the results of Sabeen *et al* [18].

5. Conclusions

In this paper, we have investigated the effect of adiabatic trapping of electrons on the linear and non-linear behavior of CKAAWs. These waves have not been investigated before for a partially degenerate plasma in the presence of a quantizing magnetic field. Since these waves are expected to be found in dense astrophysical environments which have strong ambient magnetic field and maybe partially degenerate. Taking Landau quantization into account may lead to more practical applications and to a better understanding of the formation of non-linear structures in degenerate plasmas. We have observed through Sagdeev potential approach that solitary structures exist only within a specific range of Alfvenic Mach numbers, and this range varies with the change of other parameters, including the angle of propagation. This result was confirmed by using non-linear dynamical analysis. We have shown the existence of solitary pulses by obtaining homoclinic orbits for certain parameters, and in general we observe the existence of nonlinear periodic waves.

We note that had we Taylor expanded the expression which yields Sagdeev potential in equation (15), we would have clearly seen the competition between dispersion and non-linearity that can yield a KdV equation. We have kept the problem general by preserving the degree and form of non-linearity in equation (1).

Acknowledgments

One of us (MTA) gratefully acknowledges the partial support provided by ORIC FCC.

Data availability statement

No new data were created or analysed in this study.

Declaration

Ethical approval

Not applicable as no human/animal studies are involved.

Competing interests

No, I declare that the authors have no competing interests of a financial or personal nature and in accordance with, or other interests that might be perceived to influence the results and/or discussion reported in this paper.

Authors contribution

M T Asam, S A H Bukhari and H A Shah, W Masood wrote the main manuscript Zeeshan Iqbal, L Z Kahlon did the numerical work and prepared the figures. All the authors reviewed the manuscript.

Funding

Not applicable as no funding has been received.

Availibility of data and materials

Not Applicable

ORCID iDs

H A Shah https://orcid.org/0000-0003-1236-8825
L Z Kahlon https://orcid.org/0000-0002-5517-6172

References

[1] Ang L, Kwan T and Lau Y 2003 *Phys. Rev. Lett.* **91** 208303
[2] Yang Q, Dai C, Wang Y and Zhang J 2005 *J. Phys. Soc. Jpn.* **74** 2492–5
[3] Killian T C 2006 *Nature* **441** 297–8
[4] Markowich P A, Ringhofer C A and Schmeiser C 2012 *Semiconductor Equations* (New York: Springer Science & Business Media)
[5] Craighead H G 2000 *Science* **290** 1532–5
[6] Shapiro S L and Teukolsky S A 2008 *Black Holes, White Dwarfs, and Neutron Stars: The Physics of Compact Objects* (New Jersey: Wiley)
[7] Goldman I 1947 *Zh. Eksp. Teor. Fiz.* **17** 681–5
[8] Klimontovich I U r L v 1952 *Concerning the Spectra of Systems of Interacting Particles* (US: Atomic Energy Commission)
[9] Bohm D and Pines D 1953 *Phys. Rev.* **92** 609–25
[10] Tsintsadze N L and Tsintsadze L N 2009 *Presented at the AIP Conf. Proc. (unpublished)*
[11] Shah H, Qureshi M and Tsintsadze N 2010 *Phys. Plasmas* **17** 032312
[12] Shah H, Masood W, Qureshi M and Tsintsadze N 2011 *Phys. Plasmas* **18** 102306
[13] Shah H, Iqbal M, Tsintsadze N, Masood W and Qureshi M 2012 *Phys. Plasmas* **19** 092304
[14] Ayub M, Shah H and Qureshi M 2011 *Phys. Scr.* **84** 045505
[15] Lifschitz E M and Pitajewski L P 1981 *Physical Kinetics* (Oxford: Pergamon) (*Course of Theoretical Physics*) 1st 10
[16] Landau L D and Lifshitz E M 1969 *Statistical Physics Course of theoretical physics* (Oxford: Pergamon) (*Course of Theoretical Physics*) 2nd 5
[17] Abdikian A, Saha A and Alimirzaei S 2020 *Journal of Taibah University for Science* **14** 1051–8
[18] Sabeen A, Shah H, Masood W and Qureshi M 2015 *Astrophys. Space Sci.* **355** 225–32
[19] Shah H, Masood W and Ali Z 2013 *Phys. Plasmas* **20** 032301
[20] El-Monier S and Atteya A 2022 *Waves Random Complex Medium* **32** 299–317
[21] El-Taibany W, Atteya A and El-Labany S 2018 *Phys. Plasmas* **25** 083704
[22] Tsintsadze N, Shah H, Qureshi M and Tagviashvili M 2015 *Phys. Plasmas* **22** 022303
[23] Cramer N F 2011 *The physics Of Alfvén Waves* (New Jersey: Wiley)
[24] Hasegawa A and Mima K 1976 *Phys. Rev. Lett.* **37** 690
[25] Yu M Y and Shukla P K 1978 *Physics of Plasmas* **21** 1457
[26] Barik K, Singh S and Lakhina G 2021 *Astrophys. J.* **919** 71
[27] Barik K, Singh S and Lakhina G 2019 *Phys. Plasmas* **26** 112108
[28] Wahab M A 2005 *Solid State Physics: Structure and Properties of Materials* (Oxford: Alpha Science Int'l Ltd)
[29] Saha A and Banerjee S 2021 *Dynamical Systems and Nonlinear Waves in Plasmas* (Boca Raton, Florida: CRC Press)
[30] Koester D and Chanmugam G 1990 *Rep. Prog. Phys.* **53** 837
[31] Eliasson B and Shukla P 2011 *EPL (Europhysics Letters)* **97** 15001
[32] Yadav K, Prasad A and Shrimali M D 2018 *Phys. Lett. A* **382** 2127–32
[33] Perko L 2013 *Differential Equations And Dynamical Systems* (New York: Springer Science & Business Media)
[34] Kakati H and Goswami K 1998 *Phys. Plasmas* **5** 4229–34